RADC-TR-77-179
Final Technical Report
May 1977

(12)

TEMPERATURE COMPENSATED PIEZOELECTRIC MATERIALS

Materials Research Laboratory
The Pennsylvania State University

Approved for public release; distribution unlimited

Sponsored by
Defense Advanced Research Projects Agency
DARPA Order No. 2826

ROME AIR DEVELOPMENT CENTER
AIR FORCE SYSTEMS COMMAND
GRIFISS AIR FORCE BASE, NEW YORK 13441

TEMPERATURE COMPENSATED PIEZOELECTRIC MATERIALS

Contractor: The Pennsylvania State University
Contract Number: F19628-75-C-0085
Effective Date of Contract: 31 July 1975
Contract Expiration Date: 31 March 1977
Program Code Number: 5D10
Period of Work Covered: 1 January 75 - 31 December 76
Principal Investigators: G. R. Barsch, (814) 865-1657
K. E. Spear, (814) 865-1198
Project Engineer: Paul H. Carr (617) 861-2527

This report has been reviewed and is approved for publication.

APPROVED:

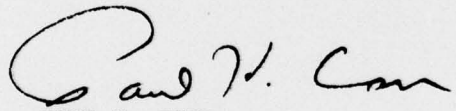

PAUL H. CARR
Project Engineer

APPROVED:

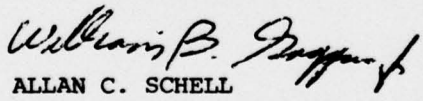

ALLAN C. SCHELL
Acting Chief, Electromagnetic Sciences Division

SECURITY CLASSIFICATION OF THIS PAGE (When Data Entered)

(19) REPORT DOCUMENTATION PAGE	READ INSTRUCTIONS BEFORE COMPLETING FORM
1. REPORT NUMBER (18) RADC-TR-77-179 / 2. GOVT ACCESSION NO.	3. RECIPIENT'S CATALOG NUMBER
4. TITLE (and Subtitle) (9) Semi-annual technical rept. (6) TEMPERATURE COMPENSATED PIEZOELECTRIC MATERIALS	5. TYPE OF REPORT & PERIOD COVERED No. Final 4 Final, 1 January 75-31 December 76
	6. PERFORMING ORG. REPORT NUMBER Semi-Annual Tech Rept. No.4
7. AUTHOR(s) (10) G. R. Barsch, K. E. Spear	8. CONTRACT OR GRANT NUMBER(s) (15) F 19628-75-C-0085, DARPA Order-2826
9. PERFORMING ORGANIZATION NAME AND ADDRESS Materials Research Laboratory, The Pennsylvania State University, University Park, Pennsylvania 16802	10. PROGRAM ELEMENT, PROJECT, TASK AREA & WORK UNIT NUMBERS PE 61101F (16) 2826 T&WU n/a
11. CONTROLLING OFFICE NAME AND ADDRESS Defense Advanced Projects Agency, 1400 Wilson Blvd., Arlington, VA 22209	12. REPORT DATE (11) May 1977
	13. NUMBER OF PAGES (12) 38 p.
14. MONITORING AGENCY NAME & ADDRESS(if different from Controlling Office) Deputy for Electronic Technology (RADC/ETEM), Hanscom AFB MA 01731, Contract Monitor, Paul H. Carr (ETEM)	15. SECURITY CLASS. (of this report) Unclassified
	15a. DECLASSIFICATION/DOWNGRADING SCHEDULE

16. DISTRIBUTION STATEMENT (of this Report)

APPROVED FOR PUBLIC RELEASE; DISTRIBUTION UNLIMITED

DDC RECEIVED SEP 19 1977 B

17. DISTRIBUTION STATEMENT (of the abstract entered in Block 20, if different from Report)

18. SUPPLEMENTARY NOTES

This work is sponsored by the Defense Advanced Projects Agency; DARPA Order No. 2826.

19. KEY WORDS (Continue on reverse side if necessary and identify by block number)

Crystal Growth; Ultrasonics; Elastic Constants; Thermoelastic Constants; Piezoelectric Constants; Temperature Compensated Materials; Surface Acoustic Devices; Eucryptite; Lead Potassium Niobate; Berlinite; Barium Germanium Titanate; Barium Silicon Titanate; Lithium Metasilicate; Bismuth Molybdate

20. ABSTRACT (Continue on reverse side if necessary and identify by block number)

In order to search for new temperature compensated materials for surface acoustic wave (SAW) devices with low ultrasonic attenuation and high electromechanical coupling, the following experimental and theoretical investigations were carried out:

DD FORM 1 JAN 73 1473 EDITION OF 1 NOV 65 IS OBSOLETE S/N 0102-014-6601

Unclassified

SECURITY CLASSIFICATION OF THIS PAGE (When Data Entered)

278870

(1) Extensive crystal growth investigations were carried out for β-$LiAlSiO_4$ (β-eucryptite), $Pb_2KNb_5O_{15}$, Li_2SiO_3, $Ba_2Si_2TiO_8$, $Ba_2Ge_2TiO_8$ and Bi_2MoO_6, using Czochralski, Bridgman or flux-pulling methods. For β-$LiAlSiO_4$ and $Pb_2KNb_5O_{15}$ single crystal specimen of sufficient size and quality for physical property measurements (5 to 10 mm linear dimensions) were obtained. The crystals obtained for the other materials were either smaller (millimeter size) or showed cracking, twinning, or the presence of inclusions.

(2) The single crystal elastic constants, the piezoelectric constants, and the temperature derivatives of these quantities have been measured by means of the ultrasonic pulse superposition method for β-$LiAlSiO_4$, α-$AlPO_4$ (α-berlinite), and $Pb_2KNb_5O_{15}$. For β-$LiAlSiO_4$ the pressure coefficients of the elastic constants were also measured. For α-$AlPO_4$ and for $Pb_2KNb_5O_{15}$ the thermal expansion behavior, and for $Pb_2KNb_5O_{15}$ the dielectric properties and the composition dependence of the ferroelectric Curie temperature were also investigated.

(3) The direction dependence of the resonance frequency and of the ultrasonic delay time, of their temperature coefficients, and of the electromechanical coupling factor was investigated theoretically with the above property data as input. β-$LiAlSiO_4$ was found to be almost temperature compensated for bulk waves, but to show smaller electromechanical coupling than α-quartz. For α-$AlPO_4$ temperature compensated directions for bulk waves with orientations similar to those for the AT and BT cuts in α-quartz, but with electromechanical coupling factors 2.5 times larger than for α-quartz were found. For $Pb_2KNb_5O_{15}$ the available data suggest the existence of temperature compensated directions with coupling factors comparable to, or larger, than for α-$AlPO_4$.

(4) The capability for measuring piezoelectric constants by means of x-rays has been developed. The theoretical equations required for the experimental determination of the complete set of piezoelectric constants by measuring the changes of the Bragg angles induced by an electric field have been derived for all 20 crystal classes exhibiting the piezoelectric effect. The method has been applied to the measurement of the piezoelectric strain constant d_{11} of α-$AlPO_4$. Preliminary results indicate that this constant (and consequently the electromechanical coupling factor) could be about 20 to 30 percent larger than the value obtained from the ultrasonic measurements.

ACKNOWLEDGMENTS

The authors gratefully acknowledge support of this work from the DEFENSE ADVANCED PROJECT AGENCY under DARPA Order No. 2826.

The authors would also like to thank their colleagues and collaborators for their participation in this work: Dr. L. Drafall for most of the crystal growth work, Dr. L. Bonczar for the crystal growth of and the property measurements on β-eucryptite, Mr. W. F. Regnault for the crystal growth of and the property measurements on lead potassium niobate, and Dr. Z. P. Chang for the property measurements on berlinite. Our thanks are extended to Professor R. Roy for supplying a single crystal specimen of berlinite, grown at the U.S. Signal Corps Laboratories, Fort Monmouth, New Jersey.

Finally, we would like to express our appreciation to the Contract Monitor, Dr. P. H. Carr, Rome Air Development Center, for initiating our search for new temperature compensated materials and for his encouragement throughout this work.

TEMPERATURE COMPENSATED PIEZOELECTRIC MATERIALS

TABLE OF CONTENTS

1. Technical Summary

1.1 Technical Problem

The objective of the research pursued under this contract was to find temperature compensated materials for use in surface acoustic wave (SAW) signal processing devices, i.e. materials with large electromechanical coupling, low ultrasonic attenuation and a vanishingly small temperature coefficient of the delay time for surface acoustic waves. The primary goal was to find materials with electromechanical coupling factors substantially larger than for α-quartz, which is at present the most widely used substrate material in temperature compensated SAW devices.

1.2 Methodological Approach

The research performed consisted of

(I) both exploratory and systematic crystal growth studies on a variety of materials which were expected to possess temperature compensated crystallographic directions and which had been selected earlier under AFCRL Contract F19628-73-C-108 on the basis of certain heuristic criteria (Barsch and Newnham, 1975),

(II) measurement of the single crystal elastic, thermoelastic, piezoelectric and dielectric properties of several promising candidate materials for which suitable single crystals were obtained, and

(III) the theoretical determination of temperature compensated crystallographic directions for ultrasonic bulk waves and their associated electromechanical coupling factors from the experimental data obtained under (II).

Based on the results obtained under (II) and (III) the existence of temperature compensated cuts for ultrasonic surface waves for the materials studied and their suitability for SAW devices was investigated by the scientific staff of the Rome Air Development Center under supervision of the Contract Monitor, Dr. P. E. Carr.

1.3 Technical Results

1.3.1 Crystal Growth

Crystal growth research has been performed on the following promising candidate materials:

(1) β-$LiAlSiO_4$

(2) $Pb_2KNb_5O_{15}$

(3) $Ba_2Si_2TiO_8$

$Ba_2Ge_2TiO_8$

(4) Bi_2MoO_6

(5) Li_2SiO_3

Sufficiently large and high quality single crystal boules suitable for the physical properties measurements were obtained for β-eucrystite,* β-$LiAlSiO_4$, and lead potassium niobate,* $Pb_2KNb_5O_{15}$. β-eucryptite was grown by the flux method* and yielded single crystals with linear dimensions up to 10 mm and volumes up to about 200 mm^3. Lead potassium niobate was grown by the Czochralski method,* but the boules had a strong tendency to crack. The cracking problems in $Pb_2KNb_5O_{15}$ were examined as a function of the variables: liquid composition, cooling rates of grown crystals, size of crystals, and the design of the heat shields above the crucible. No major solution to this cracking problem was found, but a few fairly large crack-free pieces have been obtained from some of the boules. The largest single crystal specimen that could be prepared from a boule consisted of a rectangular parallelepiped 4.1 x 2.9 x 2.7 mm^3.

Boules of $Ba_2Si_2TiO_8$ were pulled both from stoichiometric melts and from TiO_2-rich melts. However, good quality crystals were not obtained in either case. Although a single crystal boule of $Ba_2Ge_2TiO_8$ of about 10 mm diameter could be grown, its core region contained a high concentration of crystal imperfections. X-ray and hot-stage microscopic studies show that the as grown boules contain microtwins which would require strain-annealing in attempts to obtain suitable specimens for the ultrasonic measurements of elastic constants. Moreover, x-ray data on $Ba_2Ge_2TiO_8$ indicate its symmetry is monoclinic rather than orthorhombic. Therefore, crystal growth efforts on these materials was discontinued in order to focus attention on other materials which appear to promise a more rapid payoff.

Crystal growth experiments were initiated on bismuth molybdate, Bi_2MoO_6. Its peritectic melting behavior required using a flux-pulling method with MoO_3-rich solutions. Although cracking has been a problem as with the other oxide crystals, special efforts to maintain stable thermal conditions during growth and cooling

*This work was begun under a previous contract (F19628-73-C-0108)

resulted in obtaining crack-free sections of 2 to 3 mm across and about 3 mm long.

With lithium metasilicate, Li_2SiO_3, difficulties were encountered because of supercooling of the melt and cracking of the boules. Only polycrystalline boules have been obtained so far.

1.3.2 Physical Property Measurements and Suitability for Temperature Compensated SAW Devices

The independent single crystal zero-field elastic constants $c^E_{\mu\nu}$, the piezoelectric stress constants $e_{i\mu}$, and the temperature derivatives of these quantities have been measured ultrasonically by means of the pulse superposition method for β-eucryptite, β-$LiAlSiO_4$, for α-berlinite,* α-$AlPO_4$, and for lead potassium niobate, $Pb_2KNb_5O_{15}$. For β-eucryptite the pressure derivatives of the elastic constants were also measured. For berlinite and for lead potassium niobate the thermal expansion behavior, and for lead potassium niobate the dielectric properties and the composition dependence of the ferroelectric Curie temperature were also investigated. An independent experimental determination of the piezoelectric constants by means of x-rays was begun for berlinite.

1.3.2.1 β-Eucryptite

β-eucryptite exhibits the most unusual behavior in that both the temperature coefficients and the pressure coefficients of all five independent elastic constants are negative. Because of the anomolously large negative linear thermal expansion coefficient in the direction of the hexagonal axis the angular dependence of the temperature coefficients of the ultrasonic bulk wave delay time exhibits sharp minima, which correspond to very small positive values of the temperature coefficients. Thus for bulk waves β-eucryptite is almost a temperature compensated material. It has been shown by O'Connell and Carr (1977) that for surface acoustic waves temperature compensated directions do exist in β-eucryptite. Although for these directions the piezoelectric coupling factor is two times larger than for the ST cut of α-quartz the beam steering angle is as large as 18° and renders β-eucryptite less useful than quartz. Thus β-eucryptite is not a suitable temperature compensated piezoelectric material for use either in bulk or in surface acoustic wave devices

---

*The property measurements for berlinite were begun under a previous contract (F19628-73-C-0108).

1.3.2.2 α-Berlinite

The elastic and thermoelastic behavior of α-berlinite was found to be rather similar to that of α-quartz, but its piezoelectric properties turned out to be superior to those of α-quartz. The shear modulus c_{66}^{E} and the modulus $|c_{14}^{E}|$ increase with increasing temperature, and the remaining four independent elastic constants have negative temperature coefficients. Temperature compensated cuts for the bulk wave delay time and resonance frequency were found to exist in α-berlinite with orientations very similar to those for α-quartz, but with electromechanical coupling factors up to 250 percent larger than for α-quartz (Chang and Barsch, 1976). Carr and O'Connell (1976) and Jhunjhunwala et al. (1977) have performed computer calculations with the above experimental data as input and found temperature compensated directions for surface waves with electromechanical coupling coefficients 4 times larger than for α-quartz. These results suggest that α-berlinite should be a superior substitute for α-quartz, both in bulk and surface wave signal processing devices, provided high-quality single crystals with ultrasonic attenuation comparable to that of α-quartz can be grown.

1.3.2.3 Lead Potassium Niobate

Elastic and piezoelectric properties of lead potassium niobate were first investigated by Yamada (1973; 1975) who reported opposite signs of the temperature coefficients of the resonant frequencies for different crystal-cut plates, which suggests the existence of temperature compensated cuts along intermediate directions. In addition, large electromechanical coupling factors (up to 0.73) were reported (Yamada 1973; 1975). We have measured the complete set of the elastic, piezoelectric and dielectric constants, and the temperature coefficients of these quantities, for lead potassium niobate. Our results are in qualitative agreement with those of Yamada (1973; 1975) in that the temperature coefficients of the ultrasonic delay time for propagation along different crystallographic directions are of opposite sign, and large electromechanical coupling factors are found. However, significant quantitative differences between Yamada's (1973; 1975) and our elastic and piezoelectric data were found which may be tentatively attributed to differences in the nature and chemical composition of the samples. The existence of temperature compensated directions for bulk waves could be established. The magnitude of the electromechanical coupling factor for these temperature compensated cuts is still the subject of ongoing investigations.

1.3.2.4 X-Ray Determination of Piezoelectric Constants

For assessing the suitability of a given material for bulk and surface wave applications the electromechanical coupling factor has to be calculated from the elastic, piezoelectric and dielectric constants for wave propagation along the temperature compensated directions. However, the piezoelectric constants determined by the ultrasonic pulse superposition method and by the resonance method could be subject to large uncertainties. Therefore the x-ray technique first used by Bhalla et al. (1971) has been employed to determine the piezoelectric constants of berlinite directly and independently. The theoretical equations for the x-ray determination of the complete set of the piezoelectric constants for crystals of all twenty crystal classes which exhibit the piezoelectric effect have been derived (Barsch, 1976). Preliminary experimental results indicate that the piezoelectric strain constant d_{11}, and consequently the electromechanical coupling factor for the temperature compensated directions could be as much as 20 to 30 percent larger than the ultrasonically determined value. Pending experimental substantiation of this value and independent measurement of the piezoelectric strain constant d_{14} this result supports our earlier conclusion that α-berlinite should have performance properties in temperature compensated bulk and surface wave devices superior to those of α-quartz.

1.4 DOD Implications

Present and future engineering applications of SAW devices include military (and civilian) communications and Radar systems, such as multichannel communications, secure anti-jam communication for satellites, miniature avionics and electromagnetic counter measures. The main performance limiting factor of current SAW devices is that it has not been possible to simultaneously achieve high figure of merit, which increases with increasing electromechanical coupling factor, and small temperature coefficient of time delay. For applications where temperature compensated performance is essential, as in SAW code correlators and in circulating store devices, quartz has been used as a substrate material, which has a relatively small bandwidth and figure of merit.

For two of the materials investigated under the present contract one may expect the existence of temperature compensated cuts for bulk and surface waves, with substantially larger electromechanical coupling, bandwidth and figure of merit than for α-quartz. One of the materials investigated, berlinite, was found to have

temperature compensated cuts cuts with electromechanical coupling factors for bulk waves 2.5 times larger, and for surface waves 4 times larger than quartz. The second material, lead potassium niobate, could be still better. Thus by replacing quartz as a substrate material in surface acoustic wave (SAW) devices with one of these materials insertion losses can be reduced and the operating frequency and/or bandwidth can be increased. In this manner the efficiency, reliability and capability of military communications and Radar systems utilizing SAW signal processing devices can be significantly improved.

1.5 Implications for Further Research

It has been demonstrated that the search for new temperature compensated materials with properties superior to those of α-quartz through the approach used under the present contract can be successful. One may therefore hope that a continued systematic search for new temperature compensated materials under a future contract could lead to the discovery of even more suitable materials. To this end continued crystal growth efforts are required to obtain suitable single crystals for the physical property measurements, which are necessary to assess the use of a given materials for SAW device applications.

1.6 Special Comments

No special comments are offered at this time.

2. Crystal Growth Results

Our approach was to use crystal pulling (Czochralski) and directional solidification (Bridgman) techniques for the growth of these materials whenever possible. These techniques usually yield the largest crystals with the least effort, but the compounds must melt congruently and must have reasonably low vapor pressures at the melting temperature. High temperature solution growth, i.e., flux growth was used on materials that do not meet the above requirements. A hybrid flux-pulling method was used for some of these solution grown crystals.

2.1 β-Eucryptite, β-$LiAlSiO_4$

Single crystals of β-eucryptite, with linear dimensions up to 10 mm and volumes up to about 200 mm^3 were grown* by the flux method with lithium cryolite flux (Winkler, 1948). The crystals obtained are transparent and relatively free of inclusions. Oriented crystal platelets large enough for the ultrasonic determination of the elastic, thermoelastic and piezoelectric properties could be prepared from the specimen obtained.

2.2 Lead Potassium Niobate, $Pb_2KNb_5O_{15}$

Single crystal growth experiments on lead potassium niobate have been performed* with a rf-powered A.D. Little crystal puller. Although the procedures reported by Yamada (1973) have been followed, the resulting crystal boules were cracked in many places, and the single crystal regions were twinned. Various shielding assemblies and cooling procedures have been tried without success. Several compositions either rich or poor in each of the respective components were prepared and studied in an attempt to understand more about the phase equilibria of the $PbO-K_2O-Nb_2O_5$ system, and thus understand the growth of the $Pb_2KNb_5O_{15}$ from molten compositions in this system.

In a later paper by Nakano et al. (1975) it is stated that good crystals were obtained from melts with compositions $Pb_{1.90-1.95}K_{1.2-1.1}Nb_5O_{15}$. Several runs were made using these compositions, but the results were not significantly different from those of earlier experiments.

Smaller diameter crystals were grown (6-8 mm), but cracking persisted. The shielding above the crucible was varied, and in a few runs removed, but the effects were small. By varying the content of lead oxide in the melt, a few small boules were grown in which the cracking was reduced. Several oriented and parallelepiped-shaped specimens were prepared for the ultrasonic measurements. When viewed under a polarization microscope one specimen appeared to be homogeneous and free of internal strains.

Property measurements obtained on the above lead potassium niobate specimens indicated this material may be very interesting. Therefore, a decision to terminate

---

*These crystal growth investigations were begun under a previous contract (F 19628-73C-0108).

further crystal growth efforts was reversed. Since the cracking problems with this material were not eliminated by changing various growth parameters such as composition, temperature gradients, and cooling rates, the new efforts were aimed at (1) utilizing more stable temperature conditions both during growth and during the cooling cycle, (2) maintaining the boule diameter as constant as is possible without constant-diameter-control equipment, and (3) using oriented seed crystals. These new efforts could only be carried to their initial stages during this contract.

A new rf feed-back unit for temperature control was installed on the A.D. Little crystal puller and significantly reduced fluctuations in temperatures measured by a thermocouple touching the bottom of the crucible. Diameter control was enhanced, but only a few runs on this material were made. A new temperature programmer was installed to increase our temperature stability during the cooling cycle.

Nucleation on a platinum rod results in preferred growth along the crystallographic c-axis, the direction in which cracking had been a problem. Seed crystals with different orientations were used in further attempts to eliminate or at least reduce the cracking problems, but the growth direction did not appear to change the tendency to crack. These crystal boules were pulled from the melt without problem at 2 to 4 mm/hr, and tended to exhibit facets. At high temperatures the boules appeared transparent and crack-free; cooling through the transition temperature of about 500°C apparently caused the cracking. Utilizing an after-heater cooled at 10°/hr from temperatures of about 600°C to room temperature helped to reduce the cracking but did not eliminate the problem.

2.3 Lithium Metasilicate, Li_2SiO_3

Polycrystalline Li_2SiO_3 synthesized at 900°C from Li_2CO_3 and SiO_2 was used in attempts to grow single crystals of this phase from its melt by both Bridgman and Czochralski techniques. Milky, polycrystalline boules were all that could be obtained from the Bridgman directional solidification experiments, even when slow growth rates of 0.8 mm/hr were used. The temperature gradient at the melt-crystal interface was about 25 C°/inch in these experiments.

Czochralski crystal pulling experiments on Li_2SiO_3 were performed with two different pieces of equipment. The first experiments used an Arthur D. Little model MP puller heated by an rf induction generator. Since cracking of boules persisted even after using various shielding and insulation schemes, subsequent

experiments employed an NRC puller equipped with a special platinum resistance furnace built for this puller. The furnace was equipped with a proportional controller and a Data-Trak for programmable heating and cooling cycles. A special "cover" for shielding above the crucible was fabricated so that the temperature gradients for the first three inches above the melt could be varied from about 70°/inch to 200°/inch. This cover, the stability of the furnace (less than ±1/2° fluctuations), and slow pulling rates of about 2 mm/hr greatly increased the perfection of the boules, but they remained polycrystalline. Nucleating a crystal on the platform extension to the pulling rod and the necking of crystals was a problem because of (i) viewing difficulties caused by near black-body conditions, (ii) good shielding and resultant reduced temperature gradients above the melt surface, and (iii) the extreme sensitivity of the crystal diameter to the furnace temperature. A water-cooled pulling rod used with a short platinum extension for nucleating the crystal was then installed in an attempt to avoid the supercooling problem. The nucleation on the platinum rod remained extremely difficult, and it appears that a seed crystal is required to avoid this problem.

The possibility of a phase transition causing the cracking in Li_2SiO_3 was examined by DTA and high temperature x-ray experiments. The DTA experiments showed a small endothermic peak at about 1030° and then the melting point at 1200°C. High temperature x-ray diffraction patterns taken at 835°, 1060°, and 1156° showed only the expected thermal expansion of the orthorhombic unit cell; no new peaks were observed.

2.4 Fresnoite and Derivatives, $Ba_2Si_2TiO_8$ and $Ba_2Ce_2TiO_8$

Fresnoite, $Ba_2Si_2TiO_8$

Polycrystalline starting material of barium silicon titanate (fresonite), $Ba_2Si_2TiO_8$ was synthesized by 1200°C heating of pressed pellets of the proper stoichiometric amounts of $BaCO_3$, SiO_2, and TiO_2. In growth experiments, the high melting point has caused problems in attaining sufficiently high temperatures in the center of an insulated platinum crucible without almost melting the crucible. Various heat shielding arrangements around the crucible were tried, as were various reflectors and shields above the crucible. Melting was attained and several crystal boules were obtained, but they were of poor quality and were cracked extensively.

In the second approach to the cracking problem, flux-pulling experiments were attempted since the temperature requirements are not so severe. Very small crystals

of fresnoite were grown by slow cooling of TiO_2-rich melts at the National Bureau of Standards, and our own DTA experiments indicated that additions of TiO_2 to stoichiometric fresnoite lowers the melting temperature significantly. We added various amounts of TiO_2 ranging from 5 to 30 wt% to fresnoite in our experiments, and in all instances $Ba_2Si_2TiO_8$ could be pulled from these molten solutions. However, all the crystal boules contained numerous cracks and appeared more and more milky with increasing amounts of TiO_2 in the melt. With 30 wt% excess TiO_2 the melting point was lowered about 150° so that a boule could be grown without extraneous heat shields, but the boules were still cracked. A thin slab of crystal observed under the polarizing microscope showed appreciable amounts of TiO_2 flux intergrown with fresnoite. Even with slow pulling rates of about 2mm/hr, the TiO_2 flux inclusions were still a serious problem.

In pulling from the pure melt, erosion of the platinum crucible through the formation of platinum oxides was relatively large. To avoid this problem, a few growth experiments were run in argon to see if the titanium in the compound would be reduced to a trivalent state. Some reduction may have occurred, but the problem did not look severe.

Barium Germanium Titanate, $Ba_2Ge_2TiO_8$

Our major crystal growth effort during the early part of the contract centered on barium germanium titanate, $Ba_2Ge_2TiO_8$. Both Bridgman and Czochralski growth experiments were carried out, but only the latter pulling experiments were successful.

Bridgman experiments were performed in attempts to duplicate the successful growth of $Ba_2Ge_2TiO_8$ reported by Kimura et al. (1973), but all the boules obtained were cracked and milky in color. In attempting to remedy the poor quality of material obtained, better temperature control equipment was used, four different crucible lowering rates in the range of 0.5 to 3mm/hr were tried, and temperature gradients near the freezing point both greater and smaller and greater than 30°/inch were used. However, none of these changes resulted in crystal boules of even half decent quality. The reasons for these poor Bridgman results were not clear, and the experiments were terminated in favor of pulling methods.

Czochralski crystal pulling experiments utilizing an rf-powered A.D. Little model M.P. crystal puller produced good quality single crystal boules except for a central core region which was viewed. In six of the seven growth experiments, the

crystal was nucleated on a Pt or Pt/10% Rh wire 0.030 to 0.040 inches in diameter. The nature of the necking down procedure on the shape and size of an average crystal of $Ba_2Ge_2TiO_8$ grown in these studies can be seen from the photograph shown in Figure 1. A seed crystal was used in one experiment, but the quality of the resulting crystal was worse than when nucleation on the metal wire occurred. This was in spite of the fact that the seed crystal was oriented in the same direction it was initially grown, and the seed was partially melted before the new crystal was grown.

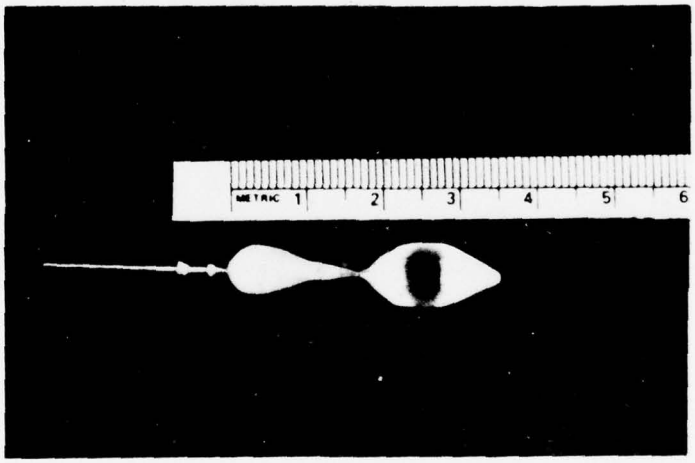

Figure 1. Typical $Ba_2Ge_2TiO_8$ Crystal Boule Pulled from Its Melt

In all of the crystals grown, a cloudy core was present which varied in size depending on the particular growth conditions. A scan with the electron microprobe across this region suggested a slight increase in germanium content, but these results are very tentative. The effects of crucible insulation and crystal rotation on the size and shape of the central core are illustrated in Figure 2, which shows the schematic cross sections of crystal boules.

During all the crystal pulling experiments on $Ba_2Ge_2TiO_8$, a small amount of material vaporized from the crucible and condensed in an amorphous state on the water-cooled chamber walls. A qualitative spectroscopic analysis of this material indicated the deposit was almost entirely germanium (probably GeO_2), with minor amounts of Pt (0.02 - 2%) and traces of Ti and Ba (<0.02%).

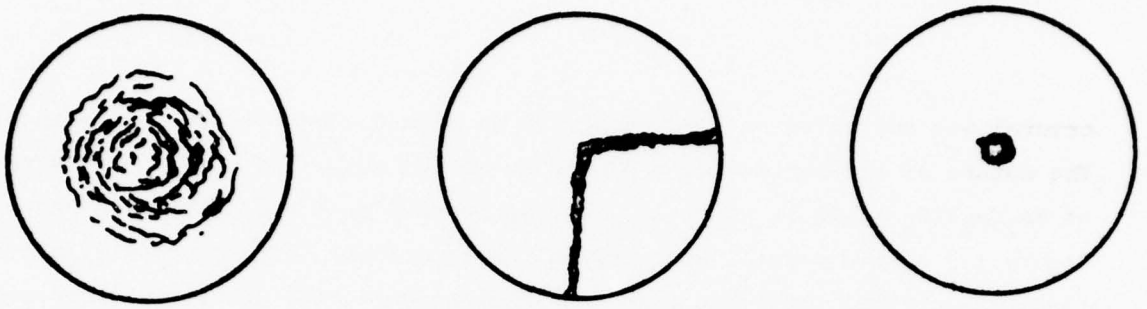

No. 2 - 20 rpm rotation
No crucible
insulation

No. 3 - 0 rpm rotation
crucible
insulated

No. 4 - 20 rpm rotation
crucible
insulated

Figure 2. Schematic Cross Sections of Crystals Grown Under Various Conditions of Crystal Rotation Rates and Crucible Insulation. The Size and Shape of the Cloudy Core Region is Indicated

Elimination of the central core imperfections in the grown crystals was attempted, but these efforts were terminated after x-ray data obtained on $Ba_2Ge_2TiO_8$ showed its crystal symmetry to be monoclinic rather than orthorhombic. Thus, thirteen independent single crystal elastic constants would be required to determine the complete set of elastic constants and their temperature coefficients. In addition, the x-ray and hot-stage microscopic studies indicate that the as-grown boules contain microtwins which would require strain-annealing in attempts to obtain suitable specimens for the ultrasonic measurements.

2.5 Bismuth Molybdate, Bi_2MoO_6

Survey crystal growth experiments on bismuth molybdate, Bi_2MoO_6, were begun during this contract. Czochralski crystal pulling methods were used since this technique usually will yield the largest crystals in the shortest period of time. However, the reported unsuccessful attempts of Miyazawa et al. (1974) to grow crystals of this phase indicated special care would be required.

Bismuth molybdate melts peritectically to give a liquid rich in molybdenum oxide and a solid rich in bismuth oxide (Chen and Smith, 1975). A liquid composition of about (45 mole% Bi_2O_3 • 55 mole% MoO_3) and a flux-pulling method allow for the pulling of Bi_2MoO_6 boules below the phase transition of this phase. Compositions

of the liquid richer in MoO_3 reduce the pulling temperature, but flux inclusions were found to be more of a problem. Vaporization of the liquid was significant but x-ray analysis of the condensed vapor showed the patterns of Bi_2MoO_6. Both high (γ) and low (γ') temperature polymorphs were observed, dependent on the temperature of the surface on which condensation occurred.

As with the other crystals studied in this program, cracking was a problem. Flux inclusions were also evident when growth conditions were not stable. These problems were attacked by using slow growth rates of 2 mm/hr, rotation rates of 20-30 rpm, temperature fluctuations on the outside of the crucible of less than ± 1°, attempts to carefully control the diameter of the boule, reduction of convection currents in the melt, and cooling of the grown boules at 8°/hr. The temperature gradients in the crucible were reduced to reduce convection currents in the melt. This was done by modifying the heat shields and by removing the insulation from the bottom of the crucible. Thus the temperature of the top and bottom of the melt were brought closer together. Boules with crack-free sections of 2 to 3 mm across and about 3 mm long were obtained as a result of these precautions.

3. Elastic, Thermoelastic, Piezoelectric and Dielectric Properties

3.1 β-Eucryptite

The five single crystal elastic constants of β-eucryptite, β-$LiAlSiO_4$ (crystal class $D_6(622)$), their temperature coefficients and their pressure coefficients have been measured by means of the ultrasonic pulse superposition method. All pressure and temperature coefficients are negative. By making measurements for 8 independent modes it was also possible to obtain the piezoelectric stiffening contribution to the effective elastic constants, as well as the temperature and pressure derivatives of this quantity. In conjunction with the dielectric constant data of β-eucryptite by Böhm (1975) it was then possible to calculate the piezoelectric constant e_{14} and its temperature coefficient from the stiffening term. All experimental results have been given in our Semi-Annual Technical Report No. 1 (Barsch and Spear, 1975).

The ultrasonic delay time t, the resonance frequency f, and the temperature coefficients of these two quantities were calculated as a function of direction. For none of the directions investigated did the temperature coefficients of the

transit time or of the resonance frequency become zero. However, the angular dependence of the temperature coefficients exhibit rather sharp minima, and the values of the temperature coefficients at these minima are very small $((1/\tau)(\partial\tau/\partial T) = 4 \times 10^{-6}(°K)^{-1}$ for $\theta = 40°$ and $\theta = 140°$, with $\phi = 0°$, 30°, 60°, where θ is the angle between the propogation electron and the c-axis, and ϕ the polar angle in the XY plane, with the X-direction along the a-axis). Thus it appears that for bulk waves β-eucryptite is almost a temperature compensated material.

The electromechanical coupling factor for the thickness-shear mode of the rotated Y-cut was calculated as a function of direction and found to show a maximum of $k = 0.027$ at an angle of 32° 40' with the Y-axis. This value is considerably smaller than the coupling factor for the temperature compensated cuts of α-quartz (0.054 for BT and 0.089 for AT). Although the value for β-eucryptite is subject to a large experimental error, because the piezoelectric stiffening term is experimentally determined as the difference between two large numbers, it is unlikely that an independent more direct determination of the piezoelectric constant e_{14} will drastically alter this result.

Another undesirable property of β-eucryptite are rather large dielectric losses parallel to the hexagonal axis; at 30°C the loss tangent decreases from a value of 1.2 for 30 Hz to a value of 0.1 for 10^5 Hz (Böhm, 1975).

Carr and O'Connell (1977) have shown on the basis of computer calculations in conjunction with the above elastic and piezoelectric data that for surface waves temperature compensated directions exist, and that the associated electromechanical coupling is two times larger than for α-quartz. However, the power flow angle of 18° is considerably larger than for quartz.

Based on the available evidence one may conclude with a high degree of probability that β-eucryptite is not a suitable temperature compensated piezoelectric material for use in bulk or surface acoustic wave devices. Because of the smallness of the electromechanical stiffening term in the Kristoffel tensor it is unlikely that this conclusion would be subject to revision as more accurate piezoelectric constant data become available.

The occurrence of all negative signs of the pressure coefficients is unique among crystalline solids, as normally pressure coefficients of elastic constants are positive, and no other crystalline material with all negative pressure

coefficients is known. The negative pressure coefficients have implications for the high-pressure phase diagrams and suggest the existence of several distinct (stable or metastable) high-pressure phases. In fact, a transformation of 8 kbar to an as yet unidentified phase has been observed by Morosin and Peercy (1975), and Neuhaus and Meyer (1965) report that between 30 to 55 kbar and at 1000°C α-eucryptite decomposes into α-spodumene and lithium aluminate.

The Grueneisen parameter of β-eucryptite has been calculated from the elastic data on the basis of the anisotropic elastic continuum model (Brugger and Fritz, 1967). The calculated value (-0.05) has the correct negative sign, reflecting the negative volume thermal expansion coefficient of β-eucryptite (Hummel, 1951; Schulz, 1974), but is smaller than the thermal value (-1.07). This suggests that the microscopic Grueneisen parameters of the phonon modes in the dispersive range (or for the optical branches) are considerably more negative than in the long-wavelength limit which is determined by the pressure coefficients of the elastic constants. Thus β-eucryptite appears to occur in an unusually metastable crystal structure which under pressure becomes unstable with respect to a variety of deformation modes.

3.2 α-Berlinite*

The six single crystal elastic constants of α-berlinite, α-$AlPO_4$, have been measured between 80°K and 298°K by the ultrasonic pulse superposition method, and the thermal expansion behavior has been determined from 293°K to 950°K by the X-ray powder diffraction method through the α-β transition at about 857°K. All results are very similar to those for α-quartz. With the exception of c^E_{66} and c^E_{14}, all elastic constants decrease with increasing temperature, but c^E_{66} and $|c^E_{14}|$ increase monotonically. As a result, temperature compensated cuts with zero temperature coefficient of the resonance frequency at 25°C are found, with orientations similar to those for the AT and BT cuts in α-quartz, but with an electromechanical coupling factor 2.5 times larger than for quartz.

Experimental details and results, and the calculated orientation dependence of the delay time, of the resonance frequency, of the temperature coefficients of these two quantitites, and of the electromechanical coupling factor for a rotated Y-cut crystal have been presented elsewhere (Chang and Barsch, 1976).

---

*These investigations were begun under a previous contract (F19628-73C-0108).

Computer calculations by Carr and O'Connell (1976) and by Jhunjhunwala et al. (1977) based on these data show that for surface waves temperature compensated cuts exist with similar orientations than for α-quartz, but with electromechanical coupling factors 4 times larger than for α-quartz. Thus in berlinite a suitable substitute material for α-quartz has been found that should exhibit superior performance characteristics in bulk and surface wave devices.

3.3 Lead Potassium Niobate

Lead potassium niobate, $Pb_2KNb_5O_{15}$, occurs in the tungsten bronze structure and belongs to the orthorhombic crystal class mm2 (C_{2v}). It is ferroelectric, with the spontaneous polarization along the b-axis and a Curie temperature of 450 ± 10°C (Nakano and Yamada, 1975). Electromechanical coupling factors as large as 0.73 have been reported (Yamada, 1973; 1975). Since the temperature coefficients of the resonant frequencies of different crystal cuts have opposite signs (Yamada, 1975) one may expect this material to be temperature compensated for intermediate directions.

Under the present contract the 3 linear thermal expansion coefficients, the density, the 9 independent elastic constants $c^E_{\mu\nu}$, the 5 piezoelectric stress constants $e_{i\mu}$ and the 3 dielectric constants ε_{ij} have been measured as a function of temperature between room temperature and 100°C. In addition, the dependence of the ferroelastic transition temperature on composition has been studied for the pseudoternary system $xK_2O + y\ PbO + z\ Nb_2O_5$ in the vicinity of the stoichiometric composition $Pb_2KNb_5O_{15}$.

The lattice parameters and the linear thermal expansion coefficients have been presented in our Semi-Annual Technical Report No. 2 (Barsch and Spear, 1976a). The lattice parameters agree well with those of Yamada (1973), but the thermal expansion coefficients differ significantly and in one instance they show even opposite signs. The density values (Barsch and Spear, 1976a) are in fair agreement with those of Yamada (1973).

The elastic and piezoelectric constants were measured by means of the ultrasonic pulse superposition method. In Table 1 the effective elastic constants obtained as eigenvalues of the Christoffel tensor with the piezoelectric stiffening term included are shown for the 18 modes corresponding to propagation directions along the x_1, x_2 and x_3 axes, and in directions forming an angle of 45° each with the x_1, x_2 axes, x_1, x_3 axes, and x_2, x_3 axes. The choice of axes follows the 1949 IRE convention. Accordingly, the x_1, x_2, x_3 axes form a right handed cartesian

Table 1. Effective Elastic Constants $\bar{c} = V^2$ for $Pb_2KNb_5O_{15}$ (Class m2m). (Elastic Constants are for Constant Field, $c_{\mu\nu} = c^E_{\mu\nu}$)

Mode No.	Direction of Propagation	Direction of Polarization	Mode Type	
1	x_1	x_1	L	c_{11}
2		x_2	S	$c_{66} + e_{16}^2/4\varepsilon_{11}$
3		x_3	S	c_{55}
4	x_2	x_1	S	c_{66}
5		x_2	L	$c_{22} + e_{22}^2/\varepsilon_{22}$
6		x_3	S	c_{44}
7	x_3	x_1	S	c_{55}
8		x_2	S	$c_{44} + e_{34}^2/4\varepsilon_{33}$
9		x_3	L	c_{33}
10	45° to x_1x_2	~45° to x_1x_2	QL	$(c_{11}+c_{22}+2c_{66})/4 + E_{13}^2+E_{23}^2+\{[(c_{11}-c_{22})/4+E_{13}^2-E_{23}^2]^2 + [(c_{12}+c_{66})/2+2E_{13}E_{23}]^2\}^{1/2}$
11		~45° to $x_1\bar{x}_2$	QS	$(c_{11}+c_{22}+2c_{66})/4+E_{13}^2+E_{23}^2-\{[(c_{11}-c_{22})/4+E_{13}^2-E_{23}^2]^2+[(c_{12}+c_{66})/2+2E_{13}E_{23}]^2\}^{1/2}$
12		x_3	S	$(c_{44} + c_{55})/2$
13	45° to x_1x_3	~45° to x_1x_3	QL	$(c_{11}+c_{33}+2c_{55})/4 + \{(c_{11}-c_{33})^2 + 4(c_{13}+c_{55})^2\}^{1/2}/4$
14		~45 to $x_1\bar{x}_3$	QS	$(c_{11}+c_{33}+2c_{55})/4 - \{(c_{11}-c_{33})^2 + 4(c_{13}+c_{55})^2\}^{1/2}/4$
15		x_2	S	$(c_{44} + c_{66})/2 + 2E_{22}^2$
16	45° to x_2x_3	~45° to x_2x_3	QL	$(c_{22}+c_{33}+2c_{44})/4+E_{21}^2+E_{31}^2+\{[(c_{22}-c_{33})/4+E_{21}^2-E_{31}^2]^2+[(c_{23}+c_{44})/2+2E_{21}E_{31}]^2\}^{1/2}$
17		45 to $x_2\bar{x}_3$	QS	$(c_{22}+c_{33}+2c_{44})/4+E_{21}^2+E_{31}^2-\{[(c_{22}-c_{33})/4+E_{21}^2-E_{31}^2]^2+[(c_{23}+c_{44})/2+2E_{21}E_{31}]^2\}^{1/2}$
18		x_1	S	$(c_{55}+ c_{66})/2$

$E_{13} = (e_{16} + 2e_{21})/4(\varepsilon_{11} + \varepsilon_{22})^{1/2}$; $E_{23} = (e_{16} + 2e_{22})/4(\varepsilon_{11} + \varepsilon_{22})^{1/2}$

$E_{22} = (e_{16} + e_{34})/4(\varepsilon_{11} + \varepsilon_{33})^{1/2}$;

$E_{21} = (e_{34} + 2e_{22})/4(\varepsilon_{11} + \varepsilon_{33})^{1/2}$; $E_{31} = (e_{34} + 2e_{23})/4(\varepsilon_{22} + \varepsilon_{33})^{1/2}$

L = Longitudinal; S = Shear; QL = Quasi-Longitudinal; QS = Quasi-Shear

coordinate system with the coordinate axes parallel to the crystallographic a, b and c-directions, which were chosen in such a manner that the lattice constants obey the inequalities $c < a < b$. According to this choice the spontaneous polarization is along the $b(x_2)$ direction, so that the point group corresponds to m2m.

Of the 18 modes listed in Table 1, three were not measured (modes numbers 3, 7 and 18) because of large ultrasonic attenutation. The measured velocity data for the remaining 15 modes were used to determine the 9 elastic constants and the 5 piezoelectric constants by means of a least squares fit, with Yamada's (1975) values for the 3 dielectric constants as input. The results (corresponding to a variance of $s^2 = 3.9 \times 10^{16} (N/m^2)$) are listed in Table 2. For comparison the results obtained by Yamada (1975) by means of the resonance technique are also included. It is apparent that most elastic and piezoelectric constants differ significantly from those reported by Yamada (1975). Although the piezoelectric constants are not quite as large as those of Yamada (1975) relatively large electromechanical coupling factors are obtained. Thus it is likely that the coupling factors for the temperature compensated directions are still larger than for α-berlinite.

The differences between the present data and those of Yamada could arise from differences in chemical composition of the samples or from the different nature of the samples. It appears that Yamada's samples were free of 180° (electrical) domains, but did contain a large amount of 90° (elastic) domains. On the other hand, the samples used in the present work were free of 90° domains, but contained 180° domains.

In an attempt to eliminate both types of domains the crystals investigated by Yamada were strain annealed in an electric field (Yamada, 1973; Nakano and Yamada, 1975). However, in this manner only the 180° domains could be removed completely, but a large amount of 90° domains remained (Nakano and Yamada, 1975). On the other hand, the crystals used in the present work are free of 90° domains and internal stresses to begin with, as could be verified by viewing the crystals under a polarizing microscope. Since the only significant effect of 180° domains is a sign reversal of some of the piezoelectric constants, and since according to Table 1 the piezoelectric constants enter the piezoelectric stiffening term in the Kristoffel tensor quadratically it is plausible to assume that the presence of 180° domains does not significantly affect the ultrasonic velocities, provided the domain dimensions are large compared with the wavelength of the ultrasonic waves. For this reason, and because of the paucity of good and sufficiently large crystal specimen available no attempt was made to remove 180° domains from the samples used for the

Table 2. Elastic Constants $c_{\mu\nu} = c^{E}_{\mu\nu}(10^{11}\ N/m^2)$ and Piezoelectric Constants $e_{i\mu}\ (C/m^2)$ of $Pb_2KNb_5O_{15}$ at 20°C Obtained from Simultaneous Least Squares Fit of all 9 Elastic Constants and all 5 Piezoelectric Constants to Measured Effective Elastic Constant Data for 15 Modes, and Comparison with Data of Yamada (1975)

	Present	Yamada
c_{11}	1.027	1.61
c_{22}	1.368	1.24
c_{33}	1.456	1.66
c_{44}	0.600	0.30
c_{55}	0.398	0.63
c_{66}	0.450	0.31
c_{12}	0.232	0.41
c_{13}	0.254	0.37
c_{23}	0.196	0.45
e_{16}	6.00	15
e_{21}	0.84	1.4
e_{22}	2.46	6.9
e_{23}	0.94	0.4
e_{34}	10.12	14

ultrasonic investigations. The presence of 180° domains (corresponding to regions with the spontaneous polarization along the positive and negative b-direction) in the specimen used in the present work could be inferred from the dielectric results obtained by the capacitance method. While the dielectric constants ε_{11} and ε_{33} (perpendicular to the direction of the spontaneous polarization) agree very well with the values given by Yamada (1975) for the free dielectric constants, the value for ε_{22} was found to be one order of magnitude larger than Yamada's value. Also no resonance behavior could be detected at 60 Hz and in the range from 10^5 to 10^7 Hz. A weak reproducible resonance curve was measured on a platelet with orientation perpendicular to the b-direction, which had been subjected at 150°C for two days to a pulsed electric field of 20 kV/cm. This suggests the presence of 180° domains in all crystals used in the present ultrasonic experiments.

In order to determine whether the differences in the elastic properties could arise from differences in stoichiometry the ferroelectric transition temperature T_c and the composition for three samples grown in this laboratory were determined. The transition temperature was measured on millimeter size single crystals by using a polarization microscope and a hot stage, and the composition was determined by means of electron microprobe analysis. The results have been presented in our Semi-Annual Technical Report No. 3 (Barsch and Spear, 1976b) and show differences of 200°C. The strong variation of T_c with composition suggests that the elastic and thermoelastic data may also significantly depend on composition. Ideally, this composition dependence should therefore be measured. Because of the difficulties of growing suitable sufficiently large single crystals for varying composition, this task was beyond the scope of the present contract, but will be tackled under a future contract from RADC.

The analysis of the temperature variation of the elastic, dielectric and piezoelectric constants, the determination of the temperature compensated directions and their associated electromechanical coupling factors, and the assessment of lead potassium niobate for bulk and surface wave devices are still in progress and will be completed under a future contract.

4. X-Ray Determination of Piezoelectric Constants

For the calculation of the electromechanical coupling factor as a function of crystallographic orientation and thus for assessing the suitability of a given material for bulk and surface wave devices the complete set of the elastic, dielectric

and piezoelectric constants must be known. The experimental determination of the piezoelectric constants from ultrasonic velocity measurements is subject to rather large experimental error since the piezoelectric stiffening term in the Kristoffel tensor is obtained as the difference between large quantities. On the other hand, results obtained by the most widely used resonance technique can be seriously in error as a result of mode coupling. For these reasons it was decided to perform independent and direct measurements of the piezoelectric constants by using the x-ray method of Bhalla et al. (1971). These authors have measured the piezoelectric constant d_{11} of α-quartz by the x-ray method and found good agreement with data obtained by other methods. Under the present contract the x-ray determination of the piezoelectric constants of berlinite was begun, and preliminary results will be reported below.

4.1 Theoretical Basis

In the x-ray method the piezoelectric constants are determined by measuring by means of x-rays the elastic strain which is induced in a crystal by an applied electric field. The theoretical equations required for the experimental determination of the complete set of piezoelectric constants from x-ray measurements have been derived (Barsch, 1976). For this purpose the expression for the quantity $(\partial\theta/\partial E)$, where θ denotes the Bragg angle and E the magnitude of an applied electric field has been calculated as a function of the field direction and the reflecting lattice plane normal. For all 20 crystal classes exhibiting the piezoelectric effect explicit expressions have been given for the longitudinal and transverse piezoelectric effect, corresponding to parallel-field and perpendicular-field reflection, respectively. For the 19 piezoelectric classes of the monoclinic, orthorhombic, tetragonal, trigonal, hexagonal and cubic systems explicit expressions for $(\partial\theta/\partial E)$ in terms of the Miller indices of the reflecting plane have been given for the simplest crystal cuts with respect to the symmetry elements present.

4.2 Preliminary Results for α-Berlinite

A pentagon-shaped X-cut platelet with face orientation, dimensions and shape as shown in Figure 3 was prepared. On the basis of the equations presented elsewhere (Barsch, 1976) the piezoelectric constant d_{11} can be determined from the electric field coefficient of the Bragg angle of the (110) reflection, and the constant d_{14} from the $(0\bar{1}4)$ and (014) reflections, with the electric field direction along the X-axis.

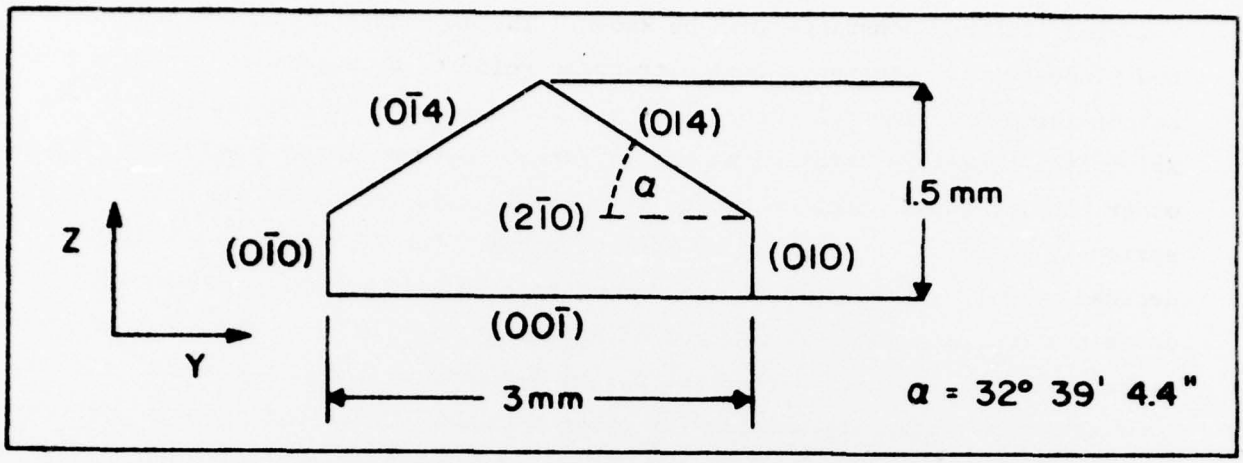

Figure 3. Dimensions, orientation and shape of X-cut platelet of berlinite sample XP1 used for x-ray determination of piezoelectric constants. The plate thickness is 1.09 mm. The orientation of the right-handed cartesian coordinate system corresponds to the 1949 IRE convention (Proc. IRE 14, 51, 1378-1395 (1949)). The pentagon shaped faces (2$\bar{1}$0) and ($\bar{2}$10) (equivalent to ($\bar{1}\bar{1}$0) and (110), respectively) were electroded.

A double crystal spectrometer was used to measure changes in the Bragg angle of the (220) reflection induced by electric field values from ± 20kV/cm to ± 30kV/cm. For an electric field of 30kV/cm the change in Bragg angle was of the order of seconds. A total of about 20 runs was made, each run consisting of the measurement of the line profile of the Bragg peak at about 70 non-equidistant values of the angle over a range of about 600 seconds, with most data points taken over a range of about 200 seconds. At each value the intensity was determined with a Geiger counter in connection with a digital readout. For each value of the electric field the line profile was least-squares fitted to a Gaussian and to a Lorentzian curve, and from the shift of the centerline with electric field the piezoelectric strain constant d_{11} was determined. The results for the measured Bragg peaks obtained in four typical consecutive runs with alternating values of the electrical field are shown in Figure 4. The least-squares fitted Lorentzian curves are also shown. The shift of the line center positions resulting from the polarity reversal of the

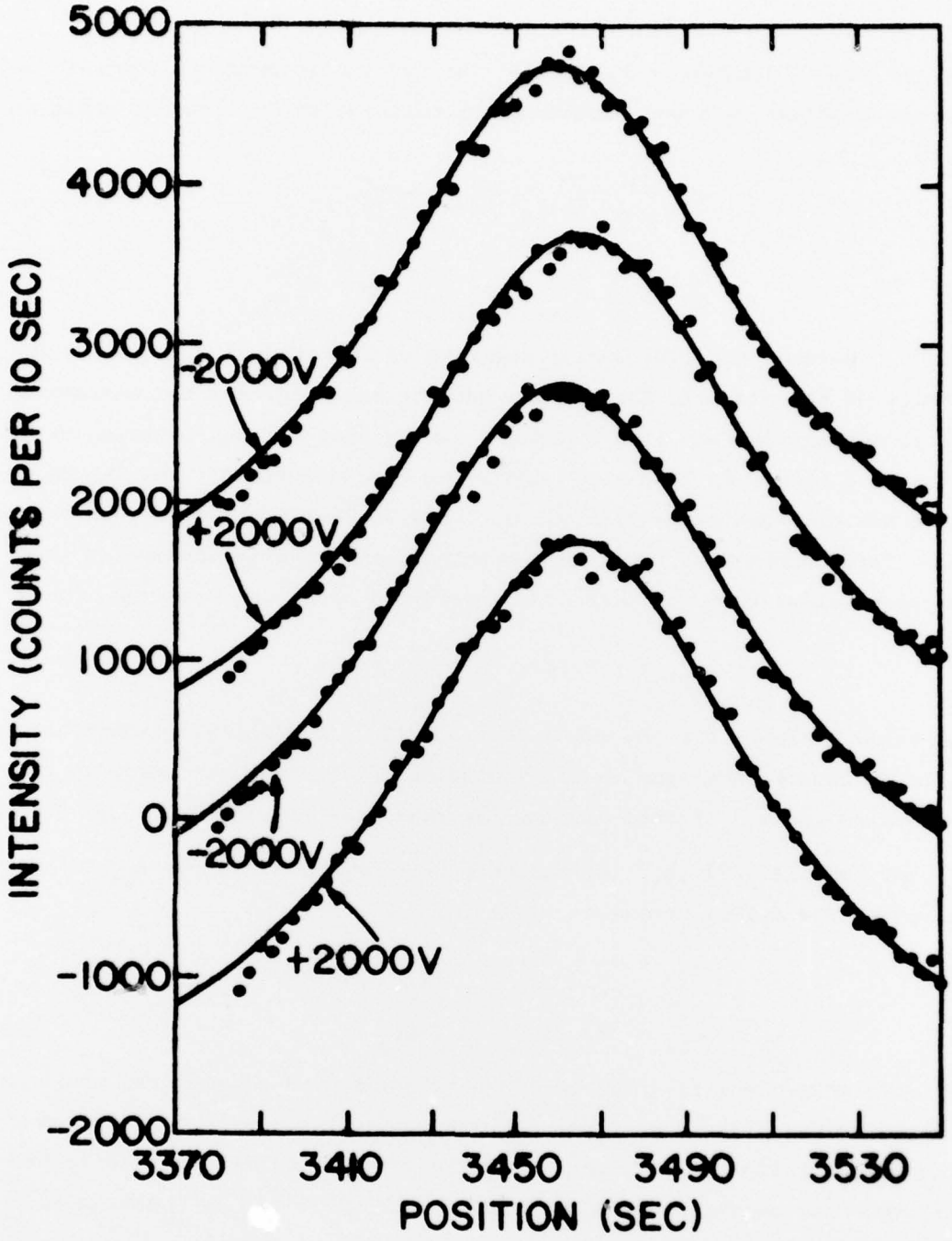

Figure 4. Line profile of (220) reflection of berlinite sample XP2 under the influence of an externally applied electric field of ± 2000V. (The curves are displaced vertically in multiples of 100 counts/second)

electric field is shown in Figure 5. The systematic drift of the data which is apparent from Figure 5 was eliminated by calculating the average shift $\Delta\theta_i$ according to

$$\Delta\theta_i = \frac{1}{2}\,(\theta^+_{i-1} + \theta^+_{i+1}) - \theta^-_i \qquad (1a)$$

and

$$\Delta\theta_i = \frac{1}{2}\,(\theta^-_{i-1} + \theta^-_{i+1}) - \theta^+_i \qquad (1b)$$

Here $\theta_i^{+,-}$ denotes the line center position of the ith run with positive (or negative) polarity of the electric field. The results obtained from the Lorentzian curve fit are systematically from 1 to 5 percent larger than for the Gaussian fit. This could be due to a change of line shape under the electric field. The values of d_{11} obtained for all runs range from 0.3 to 0.9 x 10^{-11} m/V. Many of the original runs showed large scatter of the data resulting from a faulty goniometer gear. The average obtained from the four runs considered to be the best runs is

$$d_{11} = -\ 0.60 \times 10^{-11}\ \frac{m}{V}\ \pm\ 20\% \qquad (2)$$

This value includes the low value of 0.3 x 10^{-11} m/V which was obtained on a sample of reduced size and should according to the comments below be excluded from the data analysis. If this is done the resulting average value is -0.68 x 10^{-11} m/V.

For the class 23 (D_3) the piezoelectric stress constants e_{11} and e_{14} are related to the strain constants according to

$$e_{11} = (c_{11} - c_{12})\, d_{11} + c_{14}\, d_{14} \qquad (3a)$$

$$e_{11} = 2c_{14}\, d_{11} + c_{44}\, d_{14} \qquad (3b)$$

Thus with only one strain constant determined from x-rays so far it is not possible to calculate the stress constants. However, with both stress constants e_{11} and e_{14} previously determined jointly with the elastic constants from ultrasonic velocity measurements (Chang and Barsch, 1976) it is possible to calculate the strain constants from these values, which results in

$$d_{11} = -\ 0.53 \times 10^{-11}\ \frac{m}{V} \pm 20\% \qquad (4a)$$

$$d_{14} = 0 \pm 0.3 \times 10^{-11}\ \frac{m}{V} \qquad (4b)$$

It should be noted here that the errors in (4a) and (4b) are based only on the statistical errors, but do not include systematic errors which may arise especially from the ad hoc assumptions on the dielectric constants of berlinite (Chang and

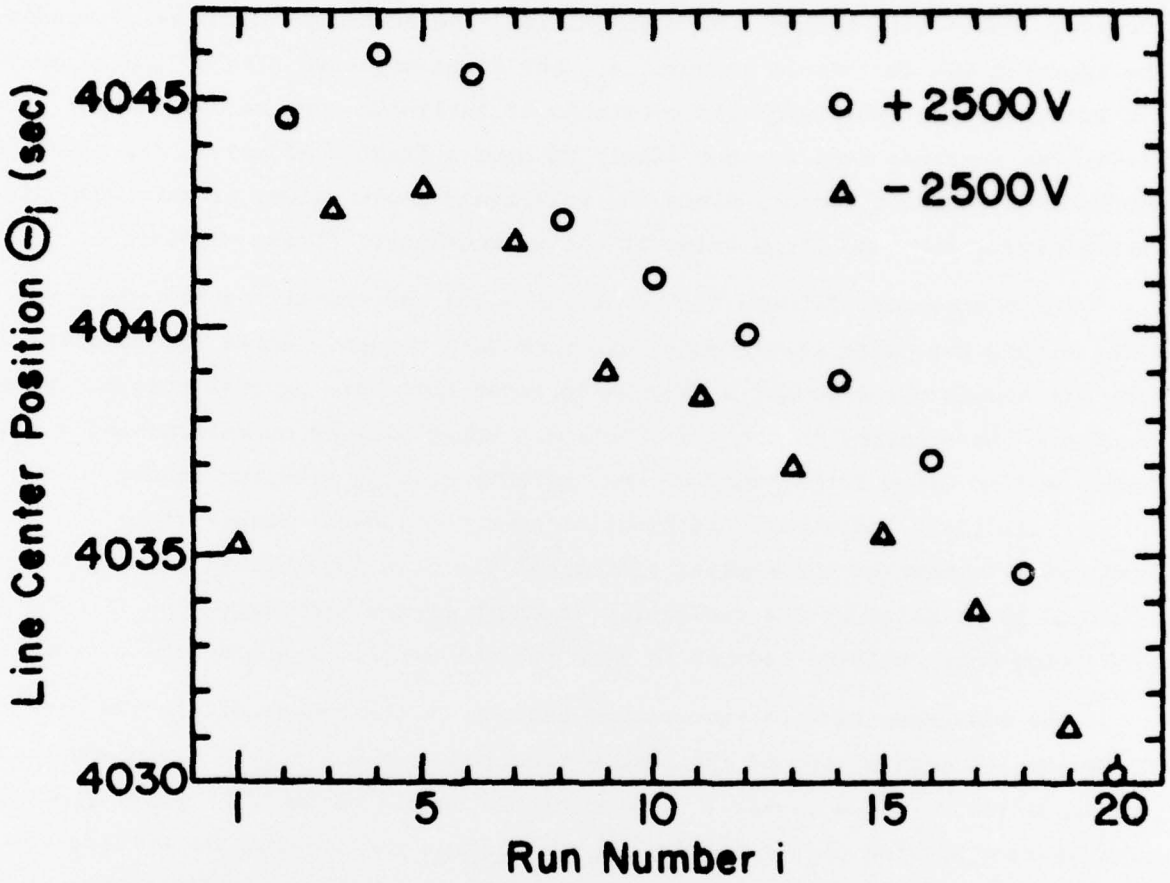

Figure 5. Line center position of (220) reflection of berlinite sample XP1 for successive runs under the influence of an externally applied electric field of ± 2500V

Barsch, 1976). The x-ray value for d_{11} is of the same order of magnitude as, but larger than the ultrasonically determined value. Thus it appears likely that the electromechanical coupling factor for the temperature compensated directions will turn out to be still larger than previously predicted (Chang and Barsch, 1976). However, for a full independent confirmation, the accuracy of the x-ray method must be improved and the strain constant d_{14} has to be measured also by the x-ray method. In addition, the two dielectric constants of berlinite must be determined. However, revisions in these data are not likely to have a drastic effect on the electromechanical coupling factor, since the relatively large values of this quantity arise mainly from the large value of the piezoelectric stress constant e_{11}.

The discrepancy between the x-ray value (2) and the ultrasonic value (4a) lies within the joint experimental error of both values. While the accuracy of the ultrasonic value cannot easily be improved there are several possible ways to increase the accuracy of the x-ray method. Especially by microfocussing of the beam, and/or using larger samples edge effects arising from the inhomogeneous electrical field and strain distribution near the lateral sample faces can be reduced. Increasing the applied electrical field is possible in principle, but limited in practice by the dielectric strength of the material. The linewidth of the Bragg peak could be reduced if more perfect single crystals were available.

The measurements were interrupted because in the course of one run dielectric breakdown through or around the sample occurred as the electric field was increased to below 3000V. As a result a segment of the sample broke off. After removing the damaged portion of the sample and repolishing and etching the surface the x-ray measurements were resumed but gave much smaller piezoelectric effects than before. Since the etch pattern obtained by etching the sample in hydrofluoric acid was drastically different on the large +X and -X faces, but uniform on either of these two faces the presence of Dauphine twins could be ruled out. In the light of Saint-Venant's principle it appears that the reduction of the piezoelectric effect is caused by edge effects since the lateral dimensions of the sample remainder (1.5 to 2 mm) are comparable to its thickness (1.09 mm). A new platelet sample has been prepared, and the measurements will be resumed under a new contract from RADC.

5. Conclusions

The results obtained under the present contract suggest that temperature compensated performance and large electromechanical coupling factors in ultrasonic bulk and surface wave devices are not mutually exclusive, and that the performance characteristics of presently used acoustic wave devices are not yet optimized with respect to the choice of the best possible material. The results indicate further that the approach used in our systematic search for new temperature compensated piezoelectric materials with larger piezoelectric coupling than α-quartz has been very successful. This approach consisted of the following four steps:

(1) Selection of promising candidate materials on the basis of heuristic criteria,

(2) Growth of single crystal specimen sufficiently large for physical property measurements,

(3) Measurement of the complete set of the elastic, piezoelectric, dielectric and thermoelastic constants,

(4) Computer calculations to determine the temperature compensated directions and their associated coupling factors for bulk and surface acoustic waves.

Based on the previous success of this approach which led to the identification of α-berlinite as a superior substitute for α-quartz one may expect that through a continued systematic search new materials with still better properties could be found.

6. Recommendations

Since α-berlinite has been found to be superior to α-quartz for bulk and surface wave applications it would seem appropriate to initiate crystal growth research and development for production of high quality (low ultrasonic attenuation) crystals of α-berlinite on a larger scale.

It appears also promising to continue the systematic search for new temperature compensated materials on the basis of the approach used previously, which could lead to the discovery of new materials with still better properties than α-berlinite. Specifically, it is recommended to continue crystal growth efforts for subsequent property measurements on the materials investigated under the present contract ($Pb_2KNb_5O_{15}$, Li_2SiO_3, $Bi_2PbNb_2O_9$, Bi_2MoO_6) and on materials selected from a previously compiled list of promising materials (Barsch and Newnham, 1975).

In order to find more precise, dependable and useful criteria for predicting new temperature compensated properties lattice dynamical investigations into the atomistic origin of positive elastic constant temperature coefficients and large piezoelectric coupling factors of known temperature compensated materials (such as α-quartz) are very desirable.

7. References

BARSCH, G.R. (1976). X-Ray Determination of Piezoelectric Constants, Acta Cryst. A32, 575-586.

BARSCH, G.R. and NEWNHAM, R.E. (1975). Piezoelectric Materials with Positive Elastic Constant Temperature Coefficients. AFCRL-TR-75-0163; Final Report on Contract No. F 19628-73-C-0108.

BARSCH, G.R. and SPEAR, K.E. (1975). Temperature Compensated Piezoelectric Materials. RADC-TR-75-609; Semi-Annual Technical Report No. 1 on Contract No. F 19628-75-C-0085.

BARSCH, G.R. and SPEAR, K.E. (1976a). Temperature Compensated Piezoelectric Materials. RADC-TR-76-184; Semi-Annual Report No. 2 on Contract No. F 19628-75-C-0085.

BARSCH, G.R. and SPEAR, K.E. (1976b). Temperature Compensated Piezoelectric Materials. RADC-TR-76-323; Semi-Annual Technical Report No. 3 on Contract No. F 19628-75-C-0085.

BHALLA, A.S., BOSE, D.N., WHITE, E.W. and CROSS, L.E. (1971). Precise X-Ray Determination of Small Homogeneous Strains Applied to the Direct Measurement of Piezoelectric Constants, phys. stat. sol. (a) 7, 335-339.

BÖHM, H. (1975). Dielectric Properties of β-Eucryptite. phys. stat. sol. (a) 30, 531-536.

BRUGGER, K. and FRITZ, T.C. (1967). Grueneisen Gamma from Elastic Data, Phys. Rev. 157, 524-531.

CARR, P.H. and O'CONNELL, R.M. (1976). New Temperature Compensated Materials with High Piezoelectric Coupling. Proceedings of the 30th Annual Frequency Control Symposium, Fort Monmouth, June 1976, pp. 129-131.

O'CONNELL, R.M., and CARR, P.H. (1977). Temperature Compensated Cuts of Berlinite and β-Eucryptite for SAW Devices. 31st Ann. Frequ. Control Symposium (June 1977).

CHANG, Z.P. and BARSCH, G.R. (1976). Elastic Constants and Thermal Expansion of Berlinite, IEEE Proc. Sonics Ultrasonics, SU23, 127-135.

CHEN, T. and SMITH, G.S. (1975). Compounds and the Phase Diagram of MoO_3-Rich Bi_2O_3-MoO_3 System. J. Solid State Chem. 13, 288-297.

GIESS, E.A., SCOTT, B.A., BURNS, G., O'KANE, D.F. and SEGMULLER, A. (1969). Alkali Strontium-Barium-Lead Niobate Systems with a Tungsten Bronze Structure: Crystallographic Properties and Curie Points. J. Am. Ceram. Soc. 52, 276-281.

HUMMEL, F.A. (1951). Thermal Expansion Properties of Some Synthetic Lithia Minerals, J. Am. Ceram. Soc. 34, 235-239.

JHUNJHUNWALA, A., VETELINO, J.F., and FIELD, J.C. (1977). Berlinite, a Temperature-Compensated Material for Surface Acoustic Wave Applications. J. Appl. Phys. 48, 887-892.

KIMURA, M., DOI, K., NANAMATSU, S., and KAWAMURA, T. (1973). A New Piezoelectric Crystal: $Ba_2Ge_2TiO_8$, Appl. Phys. Lett. 23, 531-532.

MIYAZAWA, S., KAWANA, A., KOIZUMI, H. and IWASAKI, H. (1974). Single Crystals in the Bi_2O_3-MoO_3 Binary System: Growth and Optical Properties. Mat. Res. Bull. 9, 41-52.

MOROSIN, B., and PEERCY, P.S. (1975). Pressure-Induced Phase Transition in β-Eucryptite ($LiAlSiO_4$), Physics Letters 53A, 147-148.

NAKANO, J. and YAMADA, T. (1975). Ferroelectric and Optical Properties of Lead Potassium Niobate. J. Appl. Phys. 46, 2361-2365.

NEUHAUS, A., and MEYER, H. J. (1965). Hochdruckverhalten des Eukryptits (α-$LiAlSiO_4$) und anderer oxydischer Phasen, Naturwiss. 52, 639-640.

SCHULZ, H. (1974). Thermal Expansion of Beta Eucryptite, J. Am. Ceram. Soc. 57, 313-318.

WINKLER, H.G.F. (1948). Synthese und Kristallstruktur des Eukryptits, $LiAlSiO_4$. Acta Cryst. 1, 27-35.

YAMADA, T. (1973). Single-Crystal Growth and Piezoelectric Properties of Lead Potassium Niobate. Appl. Phys. Lett. 23, 213-214.

YAMADA, T. (1975). Elastic and Piezoelectric Properties of Lead Potassium Niobate. J. Appl. Phys. 46, 2894-2898.

8. List of Publications

BARSCH, G. R., X-ray Determination of Piezoelectric Constants, Acta Cryst. A32, 575-586 (1976).

BONCZAR, L. J., Anharmonic Properties of Alkali Halides and of β-Eucryptite.* Ph.D. Thesis in Physics, The Pennsylvania State University, University Park, Pennsylvania, March 1976.

BONCZAR, L. J. and BARSCH, G. R., Pressure Dependence of Elastic Constants and Thermoelastic Properties of β-Eucryptite. To be submitted to phys. stat. sol. (1977).

CHANG, Z. P. and BARSCH, G. R., Elastic Constants and Thermal Expansion of Berlinite, IEEE Proc. Sonics Ultrasonics, SU23, 127-135 (1976).

DRAFALL, L. E. and SPEAR, K. E., Czochralski Growth of $Ba_2Ge_2TiO_8$, J. Crystal Growth 33, 180-182 (1976).

*This Ph.D. thesis was supported in part by other contracts.

METRIC SYSTEM

BASE UNITS:

Quantity	Unit	SI Symbol	Formula
length	metre	m	...
mass	kilogram	kg	...
time	second	s	...
electric current	ampere	A	...
thermodynamic temperature	kelvin	K	...
amount of substance	mole	mol	...
luminous intensity	candela	cd	...

SUPPLEMENTARY UNITS:

plane angle	radian	rad	...
solid angle	steradian	sr	...

DERIVED UNITS:

Acceleration	metre per second squared	...	m/s
activity (of a radioactive source)	disintegration per second	...	(disintegration)/s
angular acceleration	radian per second squared	...	rad/s
angular velocity	radian per second	...	rad/s
area	square metre	...	m
density	kilogram per cubic metre	...	kg/m
electric capacitance	farad	F	A·s/V
electrical conductance	siemens	S	A/V
electric field strength	volt per metre	...	V/m
electric inductance	henry	H	V·s/A
electric potential difference	volt	V	W/A
electric resistance	ohm		V/A
electromotive force	volt	V	W/A
energy	joule	J	N·m
entropy	joule per kelvin	...	J/K
force	newton	N	kg·m/s
frequency	hertz	Hz	(cycle)/s
illuminance	lux	lx	lm/m
luminance	candela per square metre	...	cd/m
luminous flux	lumen	lm	cd·sr
magnetic field strength	ampere per metre	...	A/m
magnetic flux	weber	Wb	V·s
magnetic flux density	tesla	T	Wb/m
magnetomotive force	ampere	A	...
power	watt	W	J/s
pressure	pascal	Pa	N/m
quantity of electricity	coulomb	C	A·s
quantity of heat	joule	J	N·m
radiant intensity	watt per steradian	...	W/sr
specific heat	joule per kilogram-kelvin	...	J/kg·K
stress	pascal	Pa	N/m
thermal conductivity	watt per metre-kelvin	...	W/m·K
velocity	metre per second	...	m/s
viscosity, dynamic	pascal-second	...	Pa·s
viscosity, kinematic	square metre per second	...	m/s
voltage	volt	V	W/A
volume	cubic metre	...	m
wavenumber	reciprocal metre	...	(wave)/m
work	joule	J	N·m

SI PREFIXES:

Multiplication Factors	Prefix	SI Symbol
1 000 000 000 000 = 10^{12}	tera	T
1 000 000 000 = 10^{9}	giga	G
1 000 000 = 10^{6}	mega	M
1 000 = 10^{3}	kilo	k
100 = 10^{2}	hecto*	h
10 = 10^{1}	deka*	da
0.1 = 10^{-1}	deci*	d
0.01 = 10^{-2}	centi*	c
0.001 = 10^{-3}	milli	m
0.000 001 = 10^{-6}	micro	μ
0.000 000 001 = 10^{-9}	nano	n
0.000 000 000 001 = 10^{-12}	pico	p
0.000 000 000 000 001 = 10^{-15}	femto	f
0.000 000 000 000 000 001 = 10^{-18}	atto	a

* To be avoided where possible

MISSION
of
Rome Air Development Center

RADC plans and conducts research, exploratory and advanced development programs in command, control, and communications (C^3) activities, and in the C^3 areas of information sciences and intelligence. The principal technical mission areas are communications, electromagnetic guidance and control, surveillance of ground and aerospace objects, intelligence data collection and handling, information system technology, ionospheric propagation, solid state sciences, microwave physics and electronic reliability, maintainability and compatibility.

Printed by
United States Air Force
Hanscom AFB, Mass. 01731